

Mott transition and suppression of orbital fluctuations in orthorhombic $3d^1$ perovskites

E. Pavarini,¹ S. Biermann,^{2,3} A. Poteryaev,⁴ A. I. Lichtenstein,⁴ A. Georges,^{2,3} and O.K. Andersen⁵

¹*INFM and Dipartimento di Fisica “A. Volta”, Università di Pavia, Via Bassi 6, I-27100 Pavia, Italy*

²*Laboratoire de Physique des Solides, CNRS-UMR 8502, UPS Bât. 510, 91405 Orsay France*

³*LPT-ENS CNRS-UMR 8549, 24 Rue Lhomond, 75231 Paris Cedex 05, France*

⁴*NSRIM, University of Nijmegen, NL-6525 ED Nijmegen, The Netherlands*

⁵*Max-Planck-Institut für Festkörperforschung, Heisenbergstrasse 1, D-70569 Stuttgart, Germany*

Using t_{2g} Wannier-functions, a low-energy Hamiltonian is derived for orthorhombic $3d^1$ transition-metal oxides. Correlations are treated with a new implementation of dynamical mean-field theory for non-cubic systems. Good agreement with photoemission data is obtained. The interplay of cation covalency, structural distortions, and correlation effects is found to suppress orbital fluctuations in LaTiO_3 , and even more in YTiO_3 , and to favor the transition to the insulating state.

PACS numbers: 71.27.+a, 71.30.+h, 71.15.Ap

Transition metal perovskites have been studied for decades because of their unusual electronic and magnetic properties arising from narrow $3d$ bands and strong Coulomb correlations. The $3d^1$ perovskites are particularly interesting since similar materials have very different properties: SrVO_3 and CaVO_3 are correlated metals, while LaTiO_3 and YTiO_3 are Mott insulators with gaps of respectively 0.2 and 1 eV [1, 2]. Moreover, LaTiO_3 and YTiO_3 appear to exhibit different orbital physics [3, 4].

It is believed that such properties can be described by a multi-band Hubbard Hamiltonian,

$$H = H^{LDA} + \frac{1}{2} \sum_{imm'\sigma} U_{mm'} n_{im\sigma} n_{im' -\sigma} + \frac{1}{2} \sum_{im(\neq m')\sigma} (U_{mm'} - J_{mm'}) n_{im\sigma} n_{im'\sigma}, \quad (1)$$

where $n_{im\sigma} = a_{im\sigma}^+ a_{im\sigma}$ and $a_{im\sigma}^+$ creates an electron with spin σ in a localized orbital m at site i . The direct and exchange terms of the screened *on-site* Coulomb interaction are $U_{mm'}$ and $J_{mm'}$. This Hamiltonian depends on how the ‘correlated’ orbitals are chosen. H^{LDA} is the one-electron part given by the local approximation to density functional theory (LDA), which should provide the proper material dependence. Recently it has become feasible to solve (1) using the dynamical mean-field approximation (DMFT) [5] and to obtain realistic physical properties [6]. However, so far it has been assumed that the on-site block(s) of the single-particle Green function is diagonal in the space of the correlated orbitals, and the latter have been taken as orthonormal LMTOs approximated by truncated and renormalized partial waves. Although these approximations are good for cubic systems such as SrVO_3 [7], they become increasingly worse for CaVO_3 , LaTiO_3 , and YTiO_3 whose structures are orthorhombic and increasingly distorted.

In this letter we present a new implementation of the LDA+DMFT method: By using localized Wannier functions generated by downfolding and formation of Nth-order muffin-tin orbitals (NMTOs) [8], we define a realistic Hamiltonian (1), which is solved by DMFT including

the non-diagonal part of the on-site self-energy. We apply this to the paramagnetic states of the above-mentioned $3d^1$ perovskites. Our results emphasize the interplay between structural and electronic properties. In particular, that the strong structural distortions induced by La and Y, together with correlation effects, cause the titanates to be insulating and suppress orbital fluctuations.

We first discuss the structures (Fig. 1) and our LDA bands. The cubic perovskite SrVO_3 [9] has V at the centre of a cube, O at the centres of the shared cube faces, and Sr at the shared corners. The $\frac{1}{6}$ -filled V $3d$ (t_{2g}) conduction band has a width of 2.8 eV (Fig. 2). It lies in a 3 eV gap between the occupied O $2p$ band and the empty V $3d$ (e_g) band, both of which are 5 eV wide; $\epsilon_{e_g} - \epsilon_{t_{2g}} \approx 2.8$ eV. The empty Sr $4d5s$ bands overlap the V e_g band and extend above it, while the V $4sp$ bands are far above [10]. The dispersions of the V t_{2g} and e_g bands are mainly due to hopping via O $2p$ orbitals; the t_{2g} orbitals via those in the cube faces and the e_g orbitals via the perpendicular ones. Since the former $pd\pi$ hopping integral is $\sim\sqrt{3}$ weaker than the latter $pd\sigma$ integral, the t_{2g} band is the most $3d$ -like and localized. The xy , yz and xz t_{2g} Wannier functions are not only equivalent, but also nearly decoupled from each other so that each subband is nearly 2D. The bottom of the xy band is at $(k_x, k_y) = (0, 0)$, where there is no hybridization with the O $2p$ ’s. At $(\pi, 0)$ the Ti xy orbital antibonds with its two O_x y neighbors so that the energy is increased by $\varepsilon \approx 4t_{pd\pi}^2/\Delta$, where $\Delta = \varepsilon - \epsilon_p \sim \epsilon_{t_{2g}} - \epsilon_p$. This is a saddlepoint whose nearly logarithmic 2D van Hove singularity is clearly seen in Fig. 2. At (π, π) there is additional antibonding with the two O_y x neighbors, but due to bonding interactions between the O_y x and O_x y orbitals, the energy is reduced from twice that of the saddlepoint to $8t_{pd\pi}^2/(\Delta + 2t_{pp})$. The t_{2g} band is finally modified by repulsion from the above-lying Sr $4d5s$ bands. Since the Sr $4d$ (t_{2g}) orbitals interact ($pd\sigma$) with the *same* O $2p$ orbitals as V t_{2g} ($pd\pi$), they steal O $2p$ character from the V t_{2g} band and thereby make it more narrow and symmetric around the van Hove singularity. In the expres-

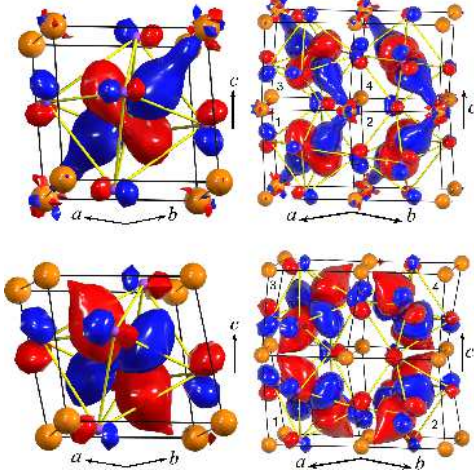


FIG. 1: $Pbnm$ primitive cell (right), subcell 1 (left), and the occupied t_{2g} orbitals for LaTiO_3 (top) and YTiO_3 (bottom) according to the LDA+DMFT calculation. In the global xyz -system, the orthorhombic translations are $\mathbf{a} = (1, -1, 0)(1 + \alpha)$, $\mathbf{b} = (1, 1, 0)(1 + \beta)$, and $\mathbf{c} = (0, 0, 2)(1 + \gamma)$, with α, β, γ small. The Ti sites 1-4 are: $\frac{\mathbf{a}}{2}$, $\frac{\mathbf{b}}{2}$, $\frac{\mathbf{a}+\mathbf{c}}{2}$, and $\frac{\mathbf{b}+\mathbf{c}}{2}$. The La(Y) ab -plane is a mirror, and so is the Ti bc -plane when combined with the translation $\frac{\mathbf{b}-\mathbf{a}}{2}$. See: <http://www.mpi-stuttgart.mpg.de/andersen/cm/0309102.html>

sions given above, this adds to Δ an energy proportional to $t_p^2 \text{Sr}_d \sigma / (\epsilon_{\text{Sr}_d} - \epsilon_{t_{2g}})$, where $\epsilon_{\text{Sr}_d} - \epsilon_{t_{2g}} \sim 3 \text{ eV}$ and $t_p \text{Sr}_d \sigma \sim t_p d\pi \sim 1.5 \text{ eV}$. Near $(0, 0)$ there is direct hopping from Sr t_{2g} to V t_{2g} . The repulsion from the Sr $4d5s$ bands makes the V t_{2g} band more 3D.

The orthorhombic $Pbnm$ structures of CaVO_3 [11], LaTiO_3 [4, 12], and YTiO_3 [13] arise from the cubic structures by tilting the MO_6 octahedra around the $x=y$ (b) axis by 9, 12, and 20° , and rotating them around the z (c) axis by 7, 9, and 13° , respectively. Neighboring octahedra have opposite tilts and neighboring c -strings opposite rotations. This leads to 4-doubling of the cell with each part being equivalent. The MO_6 octahedron is nearly perfect in CaVO_3 , but in LaTiO_3 the oxygen square in the xy -plane stretches in the a -direction by 3%, and in YTiO_3 the TiO bond in the global y - (sites 1 and 3) or x (sites 2 and 4) direction stretches by 3%. The CaV, LaTi, and YTi distances spread by ± 3 , ± 4 , and $\pm 10\%$. Most distorted are the CaO, LaO, and YO distances, some of which are 10, 13, and 21% shorter than the average. The tilts and rotations are often said to occur because the void between VO_6 octahedra has the right size for Sr^{2+} , but is too large for Ca^{2+} . TiO_6 octahedra are larger so that the void between them is far too large for La^{3+} , and even more so for Y^{3+} . This reasoning is based on oxygen-cation attraction, counter-balanced by cation hard-core repulsion (e.g. orthogonality to $\text{Sr} 3d$) and neglects oxygen-cation covalency. However, we have seen that the *excited* Sr $4d5s$ -band hybridizes with $\text{O} 2p$

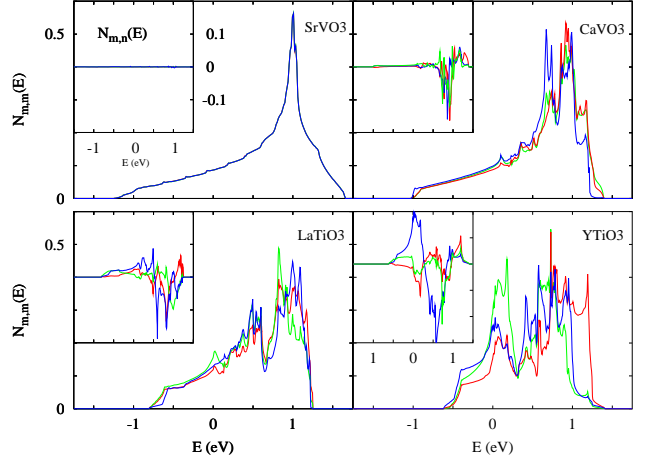


FIG. 2: t_{2g} LDA DOS matrix (states/eV/spin/band) in the Wannier representation. On-site-1 elements: $N_{xz,xz}$ (red) $N_{yz,yz}$ (green), and $N_{xy,xy}$ (blue). Insets: $N_{yz,xz}$ (red), $N_{xz,xy}$ (green), and $N_{xy,yz}$ (blue). $\epsilon_F \equiv 0$. Large $N_{m,m'}$ with $m \neq m'$ points to large off-diagonal $\Sigma_{mm'}$.

and that the oxygen-cation distance is the one most distorted in the non-cubic compounds. Moreover, when for the latter we calculate the bands in the *cubic* structure with proper cell volume, we find that the bottom of the 6 eV-wide $\text{Ca} 3d$ band is degenerate with the top of the $\text{V} 3d$ (t_{2g}) band, and that those of the 7 eV-wide $\text{La} 5d$ and the 4 eV-wide $\text{Y} 4d$ bands are degenerate with the *bottom* of the Ti t_{2g} band. This is hardly surprising, because whereas V is three rows to the right of Sr and Ca in the periodic table, Ti is *next* to La and Y. Therefore, $\epsilon_{\text{Sr}4d}/\epsilon_{\text{Ca}3d} - \epsilon_{\text{V}3d} > \epsilon_{\text{La}5d}/\epsilon_{\text{Y}4d} - \epsilon_{\text{Ti}3d}$. In addition, Sr $4d$ and La $5d$ orbitals are more extended than Ca $3d$ and Y $4d$ orbitals, whereby $t_p \text{Sr}4d \sim t_p \text{La}5d > t_p \text{Ca}3d > t_p \text{Y}4d$. We thus realize that the structural distortions are such as to increase the covalency between the $\text{O} 2p$ band and the cation sd band, which ends up *above* the t_{2g} conduction band. This leads to increasing theft of O character from the t_{2g} band, i.e. to an effective increase of Δ with the concomitant change of band-width and shape. The misalignment of the t_{2g} orbitals contributes even more to reducing the band width, from $W=3.1$ to 2.4 eV in CaVO_3 , from 2.8 to 2.1 eV in LaTiO_3 , and from 3.4 to 2.0 eV in YTiO_3 . The misalignment also leads to hybridization with the e_g band and to subband-splitting. The distortion of the octahedron as well as hybridization with the close-cation t_{2g} orbitals make the Ti t_{2g} Wannier orbitals inequivalent. A pseudo-gap appears near $\frac{2}{3}$ filling in CaVO_3 , $\frac{1}{2}$ in LaTiO_3 , and $\frac{1}{3}$ in YTiO_3 .

Before returning to this, we need to explain our NMTO+DMFT method: Since the t_{2g} band is isolated and narrow, it is a good approximation to take the correlated orbitals in (1) to be localized M-centered t_{2g} Wannier-orbitals, and to neglect the degrees of freedom from all other bands. Our Wannier orbitals are symmet-

rically orthonormalized NMTOs, which have all partial waves other than $M\,xy$, yz , and zx downfolded. Such a t_{2g} NMTO is thus dressed not only with the near oxygen and cation characters, but also with the e_g character on the neighboring and the own M sites. The latter allows the NMTO to orient itself according to its local octahedron although we take xy , yz , and zx to refer to the global cubic axes defined in Fig. 1. The localization of e.g. an xy NMTO is caused by the confinement imposed by the requirement that all its t_{2g} components on all M atoms vanish, except the on-site xy component [8]. The NMTO set completely describes the t_{2g} band, and hence form a Wannier set after orthonormalization, because its partial-wave components are solutions for the LDA potential at sufficiently many ($N+1\sim 3$) energies chosen in the t_{2g} band. Fourier transformation of the orthonormalized 12×12 NMTO Hamiltonian, $H^{LDA}(\mathbf{k})$, yields on-site blocks and hopping integrals. For the on-site Coulomb interactions, we use the common assumption that like in the isotropic case, they can be expressed in terms of two parameters: $U_{mm}=U$, $U_{mm'}=U-2J$, and $J_{mm'}=J$ for $m\neq m'$ [15]. The values of J were taken from Ref. 16. Since our Hamiltonian involves only correlated orbitals, it is not necessary to include any correction for double-counting because this is orbital-independent and therefore amounts to a simple shift of the chemical potential. H is now solved within DMFT, i.e. under the assumption that the components of the self-energy between different sites can be neglected. As a result, the self-energy can be obtained from the solution of an effective local impurity model which involves only 3 correlated orbitals. In order to study the interplay of distortions and correlation effects, *all* components of the self-energy matrix $\Sigma_{mm'}$ between different orbitals on a given site are properly treated. From this 3×3 matrix, by use of the symmetry, we construct a 12×12 block-diagonal self-energy matrix. The latter is then used together with $H^{LDA}(\mathbf{k})$ to obtain the Green function at a given \mathbf{k} -point. Fourier transformation yields the on-site block used in the DMFT self-consistency condition. The 3-orbital impurity problem is solved by a numerically exact quantum Monte Carlo (QMC) scheme based on the algorithm of Hirsch and Fye[17]. Using up to 100 slices in imaginary time allows to access temperatures down to 770 K. Typically, 750 000 QMC sweeps and 15 to 20 DMFT iterations are sufficient to reach convergence. We obtain the Green function on the imaginary time axis and calculate the spectral function using the maximum entropy technique [18].

For CaVO_3 the main effect of the orthorhombic distortion is to make the energy of the xy Wannier orbital 80 meV lower than that of the degenerate xz and yz orbitals. For LaTiO_3 and YTiO_3 the picture changes: Diagonalization of the on-site blocks of H^{LDA} in the Wannier representation gives three singly-degenerate levels with the middle (highest) being 140 (200) meV above the

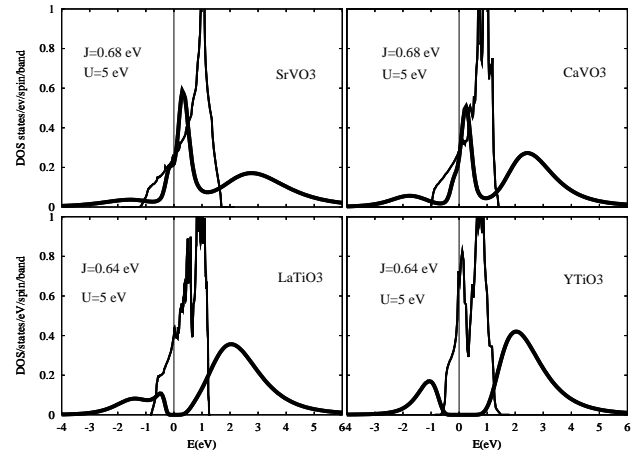


FIG. 3: DMFT spectral function at $T = 770\text{K}$ (thick line) and LDA DOS (thin line). $\mu \equiv 0$.

lowest for LaTiO_3 , and 200 (330) meV for YTiO_3 . This splitting is not only an order of magnitude smaller than the t_{2g} bandwidth, but also smaller than the subbandwidths. As a consequence, the lowest level is occupied by merely 0.45 electron in LaTiO_3 and 0.50 in YTiO_3 , and the remaining 0.55 (0.50) electron occupies the two higher levels. The linear combination of Wannier orbitals with the lowest energy is $0.604xy + 0.353xz + 0.714yz$ in LaTiO_3 and $0.619xy - 0.073xz + 0.782yz$ in YTiO_3 , on site 1. Exchanging x and y yields the results for site 2 and flipping the sign of z yields those for sites 3 and 4 (Fig. 1). The hopping integrals between the xy , xz , and yz Wannier orbitals, which in cubic SrVO_3 are independent of the orbitals and nearly diagonal, become non-diagonal in CaVO_3 , and even more so in the two insulators where the hopping is far from 2D and depends on the orbitals involved.

The LDA+DMFT calculations were performed with several values of U between 3 and 6 eV [19]. Those with $U \sim 5\text{ eV}$ reproduce the main features of the photoemission spectra for all four materials, as well as the correct values of the Mott-Hubbard gap for the insulators [2]. This is satisfying, because the value of U is expected to be similar for titanates and vanadates, although slightly larger for the latter [16]. In Fig. 3 we show the DMFT spectral functions together with the LDA total DOS. For cubic SrVO_3 we reproduce the results of previous calculations [7, 20]: the lower Hubbard band (LHB) is around -1.8 eV and the upper Hubbard band (UHB) around 3 eV . Going to CaVO_3 , the quasiparticle peak loses weight to the LHB, which remains at -1.8 eV , while the UHB moves down to 2.5 eV . These results are in good agreement with photoemission data[21] and show that SrVO_3 and CaVO_3 are rather similar, with the latter slightly more correlated. Similar conclusions were drawn in Ref. 7. From the linear regime of the self-energy at small Matsub-

ara frequencies we estimate the quasi-particle weight to be $Z=0.45$ for SrVO_3 and 0.29 for CaVO_3 . For a \mathbf{k} -independent self-energy, as assumed in DMFT, this yields $\frac{m^*}{m} = \frac{1}{Z} = 2.2$ for SrVO_3 and 3.5 for CaVO_3 , in reasonable agreement with values obtained from optical conductivity (2.7 and 3.6) [22].

For LaTiO_3 and YTiO_3 the LHB is around -1.5 eV, in accord with photoemission [23]. Despite very similar bandwidths, the gaps are very different, 0.3 and 1 eV, and this also agrees with experiments [2]. Hence, in $3d^1$ systems the Mott transition and the gap-size depend not only on U/W , but also sensitively on bandstructure details such as the pseudogap and the splitting of the t_{2g} orbitals[24]. Diagonalization of the matrix of occupation numbers reveals that now *one* orbital per site is nearly full. In LaTiO_3 it is $0.586xy + 0.275xz + 0.762yz$, containing 0.88 electron, while in YTiO_3 it is $0.622xy - 0.029xz + 0.782yz$, containing 0.96. This orbital (Fig. 1, left) is nearly identical with the one obtained from the LDA as having the lowest energy. The positive (blue) lobes have bonding $3z_{111}^2 - 1 = (xy + xz + yz)/\sqrt{3}$ character on the nearest cations –those along [111]– and the negative (red) lobes have bonding xy character on the next-nearest cations –those along [1-11]– whose oxygen surrounding is favorably oriented for this type of bond. The former type of cation covalency[14] dominates in LaTiO_3 , while the latter dominates in YTiO_3 where the shortest Y-O bond is merely 10% longer than the Ti-O bond. Hence, the difference seen between the orbital orders in the two compounds (Fig. 1, right side) merely reflects the extent to which the orbital has the bc -plane as mirror ($x \leftrightarrow y$), and the two different distortions of the oxygen square reflect rather than cause the different orbital orders. E.g. the pseudogap in YTiO_3 is *not* caused by the AF alternation of the yz and xz orbitals. Since our LaTiO_3 orbital extends towards the nearest La^{3+} ions and avoids the O^{2-} ions, it is roughly similar to the lowest orbital obtained from an accurate point-charge model[4]. Our YTiO_3 orbital is similar to the one with the highest occupancy (0.67 electrons) obtained in a spin-polarized GGA calculation[25], and has been confirmed by NMR[26] and neutron scattering[27]. However, this spin-polarized calculation yielded a *metallic* ferromagnetic ground state for YTiO_3 , like the one we would get by applying Stoner theory with $I \geq 0.9$ eV to our LDA DOS, and it only slightly increased the occupation of the lowest orbital.

The *nearly complete* orbital polarization found by LDA+DMFT for the two insulators indicates that correlation effects in the paramagnetic Mott insulating state considerably enhance orbital ordering (i.e. decrease orbital fluctuations) and makes it unlikely that YTiO_3 is a realization of an orbital liquid[28]. In LaTiO_3 some orbital fluctuations are still active, although quite weak. Responsible for the insulating character is the lowering of the effective orbital degeneracy[29].

In conclusion, we have extended the LDA+DMFT method to the non-cubic case using ab-initio downfolding to obtain a low-energy Wannier Hamiltonian. By application to the Mott transition in $3d^1$ metal-oxide perovskites, we have explained the photoemission spectra and the values of the Mott gap without adjustable parameters, except a single value of U . We have found correlation effects and cation covalency, with both O and Ti, to strongly suppress orbital fluctuations in the insulating paramagnetic phase of LaTiO_3 and YTiO_3 .

We thank J. Nuss, G. Khaliullin, M. Rozenberg, E. Koch, J. Merino, and A. Bringer for useful discussions and the KITP Santa Barbara for hospitality and support (NSF Grant PHY99-07949). Calculations were performed at MPI-FKF Stuttgart and IDRIS Orsay (project No. 021393). S.B. acknowledges support from the CNRS and the EU (Contract No. HPMF-CT-2000-00658).

- [1] For a review see M. Imada, A. Fujimori , Y. Tokura, Rev. Mod. Phys. **70**, 1039 (1998).
- [2] Y. Okimoto, *et al.*, Phys. Rev. B **51**, 9581 (1995).
- [3] C. Ulrich *et al.*, Phys. Rev. Lett. **89**, 167202 (2002); G. Khaliullin, and S. Okamoto, *ibid.*, 167201 (2002).
- [4] M. Cwik *et al.*, cond-mat/0302087.
- [5] A. Georges *et al.* Rev. Mod. Phys. **68**, 13 (1996).
- [6] V. Anisimov *et al.* J. Phys.: Cond. Matt. **9**, 7359 (1997); A.I Lichtenstein *et al.*, Phys. Rev. B **57**, 6884 (1998).
- [7] I.A. Nekrasov *et al.*, cond-mat/0211508.
- [8] O.K. Andersen and T. Sasha-Dasgupta, Phys. Rev B **62**, 16219 (2000) and Bull. Mater. Sci. **26**, 19 (2003).
- [9] M.J. Rey *et al.*, J. Solid State Chem. **86**, 101 (1990).
- [10] See also K. Takegahara, J. Electron Spectrosc. and Related Phenomena **66**, 303 (1994).
- [11] M.H. Jung, and H. Nakotte, unpublished.
- [12] D.A. MacLean *et al.*, J. Solid State Chem. **30**, 35 (1979).
- [13] M. Eitel *et al.*, J. Less-Common Met. **116**, 95 (1986).
- [14] T. Mizokawa *et al.* Phys. Rev. B **60**, 7309 (1999).
- [15] R. Fresard and G. Kotliar, Phys. Rev. B **56**, 12909 (1997).
- [16] T. Mizokawa and A. Fujimori, Phys. Rev. B **54**, 5368 (1996).
- [17] J.E. Hirsch and R.M. Fye, Phys. Rev. Lett. **56**, 2521 (1986).
- [18] J.E. Gubernatis *et al.* Phys. Rev. B **44**, 6011 (1991).
- [19] The Mott transition was found to occur for $U=6$ eV in case CaVO_3 and for $U=4.45$ eV in case of LaTiO_3 .
- [20] A. Liebsch, Phys. Rev. Lett. **90**, 096401 (2003).
- [21] K. Maiti *et al.*, Europhys. Lett. **55**, 246 (2001); A. Sekiyama *et al.*, cond-mat/0206471.
- [22] H. Makino *et al.*, Phys. Rev. B **58**, 4384 (1998).
- [23] A. Fujimori *et al.*, Phys. Rev. B **46**, 9841 (1992); K. Morikawa *et al.*, Phys. Rev. B **54**, 8446 (1996).
- [24] N. Manini *et al.*, Phys. Rev. B **66**, 115107 (2002).
- [25] H. Sawada *et al.*, Physica B **237-238**, 46 (1997).
- [26] M. Itho *et al.* J. Phys. Soc. Jap. **68**, 2783 (1999).
- [27] J. Akimitsu *et al.* J. Phys. Soc. Japan **70**, 3475 (2001).
- [28] B. Keimer *et al.*, Phys. Rev. Lett. **85**, 3946 (2000); G. Khaliullin and S. Maekawa, *ibid.*, 3950 (2000).
- [29] E. Koch *et al.*, Phys. Rev. B **60**, 15714 (1999); S. Florens *et al.*, Phys. Rev. B **66**, 205102 (2002).